Trp82 and Tyr332 Are Involved in Two Quaternary Ammonium Binding Domains of Human Butyrylcholinesterase as Revealed by Photoaffinity Labeling with [^{3}H]DDF†

Florian Nachon,‡ Laurence Ehret-Sabatier,‡ Damarys Loew,§ Christophe Colas,‡ Alain van Dorsselaer,§ and Maurice Goeldner*,‡

Laboratoire de Chimie Bio-organique, UMR 7514 CNRS, Faculté de Pharmacie, Université Louis Pasteur Strasbourg, 74 route du Rhin, BP 24, 67401 Illkirch Cedex, France, and Laboratoire de Spectrométrie de Masse Bio-organique, UMR 7509 CNRS, Faculté de Chimie, Université Louis Pasteur Strasbourg, 1 rue Blaise Pascal, 67096 Strasbourg Cedex, France

Received March 9, 1998; Revised Manuscript Received May 4, 1998

ABSTRACT: Purified butyrylcholinesterase (BuChE) was photolabeled by [^{3}H]-*p*-*N*,*N*-dimethylamino benzene diazonium ([^{3}H]DDF) to identify the quaternary ammonium binding sites on this protein [Ehret-Sabatier, L., Schalk, I., Goeldner, M., and Hirth, C. (1992) *Eur. J. Biochem. 203*, 475−481]. The covalent photoincorporation occurs with a stoichiometry of one mole of probe per mole of inactivated site and could be fully prevented by several cholinergic inhibitors such as tacrine or tetramethylammonium. After complete deglycosylation of the enzyme using *N*-glycosidase F, the alkylated protein was trypsinolyzed and the digests were analyzed by HPLC coupled to ES-MS. A direct comparison of tryptic fragments from labeled and unlabeled BuChE allowed us to identify the tryptic peptide Tyr61-Lys103 as carrying the probe. Purification of the labeled peptides by anion-exchange chromatography gave a major radioactive peak which was further fractionated by reversed-phase HPLC leading to three, well-resolved, radioactive peaks. Microsequencing revealed that two of these peaks contained an overlapping sequence starting at Tyr61, while the third peak contained a sequence extending from Thr315. Radioactive signals could be unambiguously attributed to positions corresponding to residues Trp82 and Tyr332. This labeling study establishes the existence of two different binding domains for quaternary ammonium in BuChE and exemplifies additional cation/π interactions in cholinergic proteins. This work strongly supports the existence of a peripheral anionic site in BuChE, implying residue Tyr332 as a key element.

Two types of cholinesterases can be distinguished in vertebrates; acetylcholinesterase (AChE,[1] EC 3.1.1.7) and butyrylcholinesterase (BuChE, EC 3.1.1.8). These very homologous enzymes both rapidly hydrolyze the neurotransmitter acetylcholine but show distinct substrate and inhibitor selectivity (*1*). The elucidation of the 3D structure of *Torpedo* AChE (*2*) followed by the description of a series of 3D structures of enzyme−inhibitor complexes (*3*−*6*) have revealed remarkable structural features for this protein. Extensive site-directed mutagenesis and molecular dynamics experiments have tried to assess the different functional characteristics of this enzyme, including the unusual location of the catalytic triad at the bottom of a 20 Å depth (*7*, *8*). Another noteworthy feature of this protein was an allosteric regulation of its activity by molecules binding at the peripheral site located at the entrance of this cavity. The different X-ray structures also allowed us to exemplify very accurately, in a biological model, cation/π interactions (*9*, *10*) between quaternary ammonium salts and aromatic residues. The 3D structure of BuChE has not been solved yet, and most of the structure−function investigations rely on a 3D model of this protein (*11*), which is based on the 3D structure of *Torpedo* AChE. Most of these investigations are focused on the functional specificities between aligned amino acids from different ChE species.

Contrary to site-directed mutagenesis analyses, site-directed labeling experiments do not require the existence of a 3D structure or a model of a protein. They lead to structural characterizations of ligand receptor interactions in solution (*12*), and after the publication of the amino acid sequence of AchE (*13*), early structural information resulted from photoaffinity or affinity labeling experiments. These site-directed labeling experiments allowed the identification of residues from the active site, such as Phe330 (14) and Trp84 (*15*), or from the peripheral site, such as Trp279 (*16*, *17*), His280 (*18*), Tyr70, and Tyr121 (*19*), of *Torpedo* AChE. Aromatic diazonium salts proved to be particularly attractive

† This work was supported by the Centre National de la Recherche Scientifique, the Ministère de la Recherche et de la Technologie, and the European Community Biotechnology Program under Grant No. 960081.

* To whom correspondence should be adressed. E-mail: goeldner@bioorga.u-strasbg.fr.

‡ Laboratoire de Chimie Bio-organique.

§ Laboratoire de Spectrométrie de Masse Bio-organique.

[1] Abbreviations: BuChE, butyrylcholinesterase; AChE, acetylcholinesterase; PAS, peripheral anionic site; DDF, *p*-(*N*,*N*-dimethylamino)-benzenediazonium fluoroborate; THA, tacrine; DTT, dithiothreitol; NM7C, *N*-methyl-(7-dimethylcarbamoxy)quinolinium iodide; SDS, sodium dodecyl sulfate; TFA, trifluoroacetic acid; HPLC, high-performance liquid chromatography; MS, mass spectrometry; ES, electrospray; MALDI, matrix-assisted laser-desorption−ionization; PAGE, polyacrylamide gel electrophoresis.

S0006-2960(98)00536-4 CCC: $15.00
Published on Web 06/26/1998

photoaffinity probes for the structural investigations of the acetylcholine binding site on cholinergic proteins. As a remarkable example, the [^{3}H]-*p*-*N*,*N*-dimethylamino benzene diazonium salt ([^{3}H]DDF) allowed the identification of no less than eight different amino acid residues from the acetylcholine binding site on the nicotinic receptor (*12*).

In this paper, we analyzed, at the molecular level, photoaffinity labeling experiments on BuChE using [^{3}H]DDF (*20*). The specific photoincorporation of the probe allowed, after the deglycosylation of the protein, using MS methods applied on the crude tryptic digest, the identification of the tryptic fragment Tyr61-Lys103 as being alkylated by the photoprobe. In parallel, standard purification and sequencing methods lead to the unambiguous identification of the labeled amino acids Trp82 and Tyr332. These photoaffinity labeling results strongly support the existence of two distinct ammonium binding sites in BuChE, involving cation/π interactions.

MATERIALS AND METHODS

Chemicals

Dithiothreitol, tacrine, 4-vinylpyridine, and *n*-octyl-β-D-glucopyranoside were purchased from Sigma, and butyrylthiocholine iodide and 5,5′-dithiobis(2-nitrobenzoic acid) were from Aldrich. Porcine pancreatic trypsin (sequencing grade modified) was from Promega and recombinant *N*-glycosidase F from Boehringer Mannheim. *N*-Methyl-7-hydroxyquinolinium iodide and the derived dimethylcarbamic acid ester NM7C were prepared as described (*21*). Tritiated *p*-(*N*,*N*-dimethylamino) benzenediazonium ([^{3}H]DDF; 1−6.25 Ci/mmol) was prepared as previously described (*22*).

Butyrylcholinesterase Preparation

Human butyrylcholinesterase (BuChE) was purified from frozen outdated plasma (gift from the Centre de Transfusion Sanguine, Strasbourg). We used the classical two-step procedure described by Lockridge (*23*) consisting of DEAE ion-exchange chromatography followed by procainamide affinity chromatography. Protein concentration was estimated from absorbance at 280 nm ($e = 1.8$ mL mg^{-1} cm^{-1}) (*23*) using the Bradford assay (Biorad). Activity was assayed spectrophotometrically using butyrylthiocholine as the substrate (*24*). BuChE active serines were titrated using the NM7C method (*21*). The purified enzyme (400 ± 50 units/mg) can be stored at least one year at 4 °C in 50 mM phosphate buffer, pH 7.0, without loss of activity.

Photolabeling Experiments

Photolabeling of BuChE was performed as described (*20*) in 50 mM phosphate buffer, pH 7.2, by irradiation at 295 nm under energy transfer (*25*), 75 μV for 45 min at 10 °C. The total volume for each irradiation was 1.5 mL. Final concentrations were 300 μg/mL BuChE, 100 μM [^{3}H]DDF, and, in the protection experiment, 2 μM THA. After irradiation, 2 mM DTT was added to destroy unreacted [^{3}H]-DDF. An aqueous dilution−concentration procedure on CM30 filter units (Amicon) was repeated twice and removed up to 90% of the free radioactive ligand before a final lyophilization.

[^{3}H]DDF Incorporation Measurement

Aliquots of alkylated BuChE were analyzed on a 10% SDS−PAGE (*26*). The radioactivity incorporated was quantified after gel slicing, digestion, and counting (*20*).

Reduction−Alkylation

Lyophilized−alkylated BuChE (450 μg) was redissolved in 0.5 M Tris-HCl buffer, pH 8.5, containing 5 M urea and 40 mM DTT (final volume 100 μL). The sample was incubated for 1 h in the dark at 50 °C under a stream of argon. 4-Vinylpyridine was added to a final concentration of 450 mM, and incubation was prolonged for 15 min. The protein was then extensively dialyzed against 50 mM NH_4HCO_3 buffer, pH 8.

Enzymatic Deglycosylation and Proteolytic Cleavage

Reduced−alkylated BuChE was incubated at 37 °C for 16 h in 50 mM NH_4HCO_3 buffer, pH 8, containing 0.01% SDS and *N*-glycosidase F (22 units/mg BuChE). The reaction was either stopped by denaturation and analysis on an 8% SDS−PAGE to ascertain the loss of glycosylation weight or followed by addition of trypsin (w/w; 1/45) and subsequent incubation for 6 h at 37 °C. The trypsinolysis was stopped by the addition of one volume of acetonitrile and/or by acidification.

Peptide Purification

First Step. Tryptic digests were loaded onto a cation-exchange HPLC column (Waters S5SCX, 4.6 × 250 mm) equilibrated with 25 mM $AcONH_4$ buffer, pH 4.5, containing 50% acetonitrile. Peptides were eluted with a linear gradient from 0% to 40% of the equilibrating solution containing 1 M NaCl, over 40 min at a flow rate of 1 mL/min. Absorbance was monitored at 214 nm. Fractions (0.5 mL) were collected, and aliquots were assayed for radioactivity. Fractions of interest were concentrated under vacuum (Speedvac) in order to remove acetonitrile before proceeding to the next step.

Second Step. Samples were loaded onto a reversed-phase HPLC column (Vydac 218TP52, 2.1 × 250 mm) equilibrated with 95% A/5% B (solvent A, 0.1% TFA in water; solvent B, 0.085% TFA in acetonitrile). Elution was performed at a flow rate of 0.25 mL/min with a linear biphasic gradient of 5−15% B over 5 min then 15−40% B over 100 min. Absorbance was monitored at 214 nm. Fractions (0.25 mL) were collected, and those containing radioactivity were lyophilized.

Peptide Sequencing

Peptides were redissolved in 50% formic acid. Automated Edman degradation was performed on a pulse liquid automatic sequenator (Applied Biosystems Model 473A). The remaining HPLC output from each cycle was collected and counted for radioactivity quantification.

Mass Spectrometry Analyses

For mass spectrometry analysis, BuChE was photolabeled with nonradioactive DDF as described before. After reduction−alkylation steps, the samples, unlabeled (control) and labeled, were deglycosylated and trypsinolyzed replacing

0.01% SDS by 0.4% *n*-octyl-β-D-glucopyranoside during the deglycosylation procedure. Reaction was stopped by acidification (0.1% TFA) before LC/MS analysis.

Liquid Chromatography/Mass Spectrometry (LC/MS). The chromatography was carried out on an Alliance HPLC system (Waters 2690) equipped with a diode array detector (Waters 996). Absorbances were monitored with a chromatography manager Millennium (version 2.15.01). The column was a Nucleosil 300-5C18 (Macherey Nagel, 2.1 mm $\times$ 125 mm) maintained at 35 °C. The solvent system consisted of 0.1% TFA in water (solvent A) and 0.08% TFA in acetonitrile (solvent B). The elution was performed at a flow rate of 0.25 mL/min, using a multiphasic gradient of 0% B (5 min), 0−20% B (15 min), 20−50% B (70 min), and 50−80% B (5 min) successively. The column efluent was flow-splitted via a stainless steel Valco tee (Supelco) with $^1/_{15}$ directed toward the electrospray mass spectrometer by means of fused silica capillary. Fractions of residual effluent were hand-collected. Therefore, for all analyses, both UV and mass measurement detections were obtained.

Electrospray Mass Spectrometry (ESMS). The positive ES mass spectra were obtained on a VG BioQ triple quadrupole mass spectrometer (mass to charge (*m*/*z*) range 4000) upgraded by the manufacturer to a Quattro II performance (Micromass Ltd UK, Altrincham). Scanning was performed in the range 500−2000 in 6 s at an extracting cone voltage of 40 V. The mass spectrometer was externally calibrated by using horse heart myoglobin multiply charged ions and the resolution adjusted so that the peak at *m*/*z* 998 was 1.25 wide at 50% on the base.

Matrix-Assisted Laser-Desorption−Ionization Mass Spectrometry (MALDI-MS). The collected fractions were concentrated under vacuum and redissolved in 15 μL of 50% acetonitrile, 1% formic acid. Aliquots of 0.5 μL were analyzed by MALDI-MS.

The mass spectrometry experiments were performed on a Bruker (Bremen, Germany) Biflex matrix-assisted laser-desorption−ionization time-of-flight mass spectrometer with improved resolution by means of delayed-ion extraction (DE). The samples were prepared by a two-layer method described elsewhere (*27*) and desorbed/ionized using a pulsed nitrogen laser beam (λ = 337 nm) at a repetition rate of 3 Hz. All studies were performed in the linear and reflector positive mode at an acceleration potential of 20 and 19 kV, respectively. The spectra were externally calibrated using the $[M + H]^+$ ions of angiotensin II (1046.19) and ACTH 18-39 (2465.69) in the reflector mode and ubiquitin (8564.87) and cytochrome C (12361.09) in the linear mode.

RESULTS

Photolabeling of BuChE Using [^{3}H]DDF

Purified human BuChE was photolabeled by [^{3}H]DDF (100 μM) leading to a 50% inactivation after 45 min of irradiation. In the presence of 2 μM tacrine (Figure 1), BuChE was efficiently protected against this inactivation. Figure 2 shows the incorporation of [^{3}H]DDF on both monomer (85 kDa) and dimer (170 kDa) of BuChE after denaturating electrophoresis. The quantification of incorporated radioactivity allowed us to calculate a stoichiometry close to one mole of [^{3}H]DDF incorporated per inactivated site. The specificity of the labeling was demonstrated by

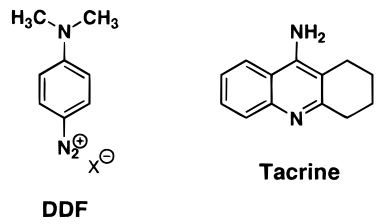

FIGURE 1: Structures of *p*-(*N*,*N*-dimethylamino)benzenediazonium and tacrine.

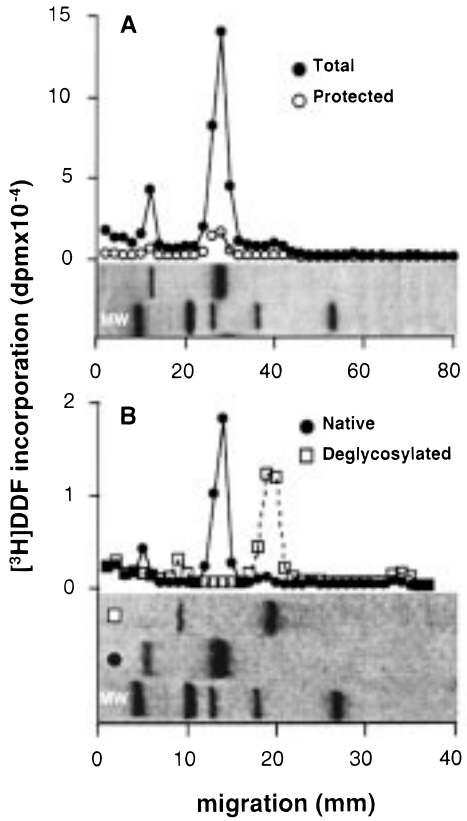

FIGURE 2: SDS−PAGE analysis of [^{3}H]DDF incorporation into BuChE upon iradiation. (A) BuChE was irradiated with [^{3}H]DDF (100 μM, 6.25 Ci/mmol) in the presence (○, protected) or absence (●, total) of tacrine (2 μM). Samples were denatured and subjected to a 10% SDS−PAGE (amount BuChE loaded, 10 μg). Molecular mass protein markers were 200, 116, 97.4, 66, and 45 kDa. The gel lanes were cut into slices which were digested and counted. (B) BuChE was irradiated with [^{3}H]DDF (100 μM, 1 Ci/mmol). After reduction−alkylation, lyophilized alkylated BuChE was (●) (or not (□)) deglycosylated. Samples were denatured and subjected to electrophoresis on a 8% SDS−acrylamide gel (amount BuChE loaded, 5 μg). The gel lanes were cut into slices which were digested and counted.

preventing the incorporation of radioactivity with tacrine (Figure 2A). When the labeled BuChE was treated with *N*-glycosidase F, the electrophoresis gel profile (Figure 2B) exhibited a shift of the protein bands concomitant with the radioactivity signals. The observed shift of 25 kDa is in agreement with a complete deglycosylation (*28*).

Mass Spectrometric Analysis of Labeled BuChE

After deglycosylation and trypsinolysis the digests were analyzed by HPLC with multiwavelength detection and coupled to ES-MS. Figure 3 shows the UV profiles of unlabeled (as control) and DDF-labeled digests. The profiles are identical along the entire chromatograms except at

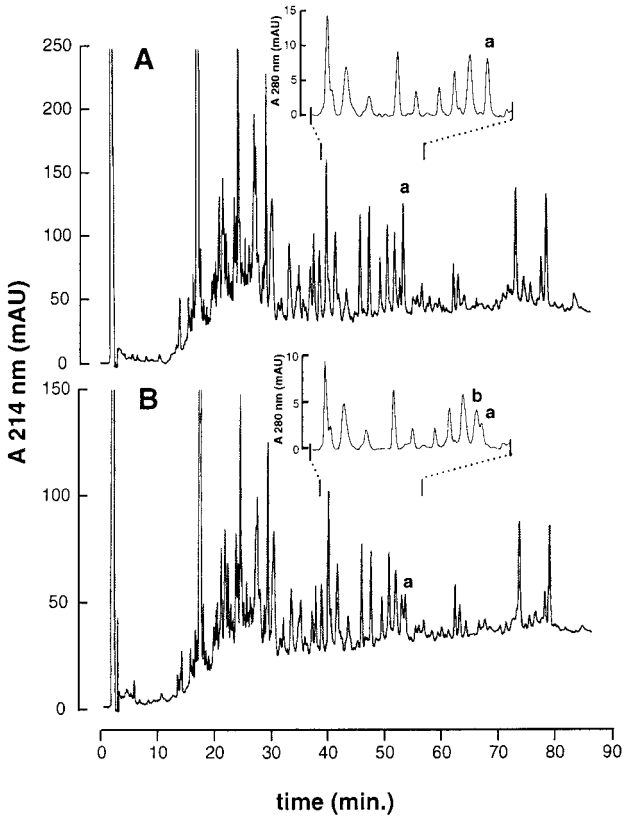

FIGURE 3: Comparison of LC/MS chromatograms from unlabeled (A) and labeled (B) trypsinolyzed BuChE. Samples of DDF-labeled and unlabeled BuChE (75 μg protein) were deglycosylated, digested, and submitted to LC/MS analysis as described in Materials and Methods. UV absorbance was monitored at 214 and 280 nm. The profiles are given at 214 nm while interesting regions are expanded and shown at 280 nm.

retention times 51−52 min. In this area, the absorbance at 214 nm of one peak (peak a) clearly decreases in the DDF-labeled digest while monitoring the absorbance at 280 nm shows a concomitant appearance of a new peak b. Figure 4 shows the mass spectra sum of peptides eluted in the ion source in this time range. Three ions (m/z = 1069.1, 1336.2, 1780.8) are present only in the labeled digest and correspond to different protonated states (respectively 5, 4, 3) of an average molecular mass of 5340.3 ± 0.6 Da. This measured molecular mass did not fit with any native tryptic peptide and was attributed to a DDF-labeled peptide. As previously indicated, with one mole of probe being incorporated per inactivated site, the difference of mass between native and labeled peptide should correspond to the mass of the incorporated label, that is, 119 Da, after substitution of a hydrogen atom by the photogenerated dimethylaminophenyl cation. Consequently, the measured mass for the labeled peptide (5340.3 ± 0.6 Da) agrees with the labeling of the parent peptide of measured average molecular mass 5221.7 ± 1.8 Da (m/z = 1045.6, 1305.9, 1741.7, Figure 4) and corresponds to the peptide Tyr61-Lys103 (calculated average mass: 5222.9 Da).

The identification of the labeled peptide was confirmed by MALDI-MS analysis of the collected HPLC fractions. The mass of the native peptide Tyr61-Lys103 could be identified in peak a, both in labeled and unlabeled digests, while the mass of the labeled peptide could be detected only in peak b of labeled digest (spectra not shown).

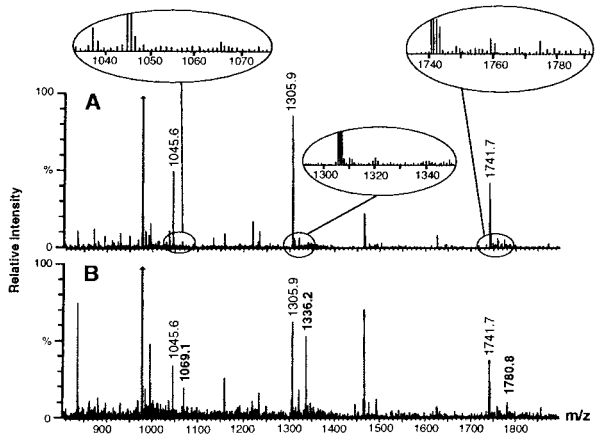

FIGURE 4: Comparison of ES/MS spectra from unlabeled (A) and labeled (B) trypsinolyzed BuChE. Spectra are shown for peptides eluting at retention time 51−52 min (Figure 3). The quoted peaks (1045.6, 1305.9, 1741.7 Da) correspond to three different charge states of a peptide which has a mass of 5221.7 ± 1.8 Da and was identified as Tyr61-Lys103. The three additional bold typed quotations in Figure 4B (1069.1, 1336.2, 1780.8 Da) show the ions corresponding to the labeled peptide (5340.3 ± 0.6 Da). Expanded spectra in Figure 4A show the absence of this peptide in the unlabeled experiment.

In conclusion the results obtained by mass spectrometry, without resorting to extensive purification of labeled peptides, indicate that the peptide Tyr61-Lys103 was specifically labeled by DDF.

Identification of [^{3}H]DDF-Labeled BuChE Residues

First attempts to purify labeled peptides were carried out without deglycosylation of the protein. After photolabeling, BuChE was trypsinolyzed and the peptides fractionated by anion-exchange chromatography (MonoQ) followed by reversed-phase HPLC. However this procedure did not lead to satisfactory results due to glycosylation heterogeneity affording complicated peptide mixtures from which we were unable to unambiguously identify the labeled residues.

Thus, BuChE was deglycosylated before trypsinolysis, and [^{3}H]DDF-labeled peptides could then be purified by a two-step procedure. The first step was cation-exchange chromatography which had the advantage, when compared to the previously used anion exchange, to be compatible with the presence of the anionic detergent SDS used for deglycosylation. Moreover, a concentration of 50% acetonitrile was added to the elution buffer in order to obtain satisfactory yield of radioactivity elution (75%). Figure 5A shows the UV and radioactivity profiles of this chromatography. The fractions containing the major radioactive peak were further treated by simultaneous desalting and purification by reversed-phase HPLC, affording three resolved radioactive peaks 1, 2, and 3 (Figure 5B). The other minor radioactive fractions (Figure 5A) were also analyzed by reversed-phase HPLC and exhibited the same radioactive peaks 1, 2, and 3 but in different relative proportions.

The three peaks 1, 2, and 3 were sequenced (Table 1). Peak 1 contained the sequence extending from Thr315, and the radioactivity was associated with Tyr332. Peaks 2 and 3 both contained sequences beginning at Tyr61 with the radioactivity associated with Trp82. These sequences were thought to be of different length due to incomplete proteolysis.

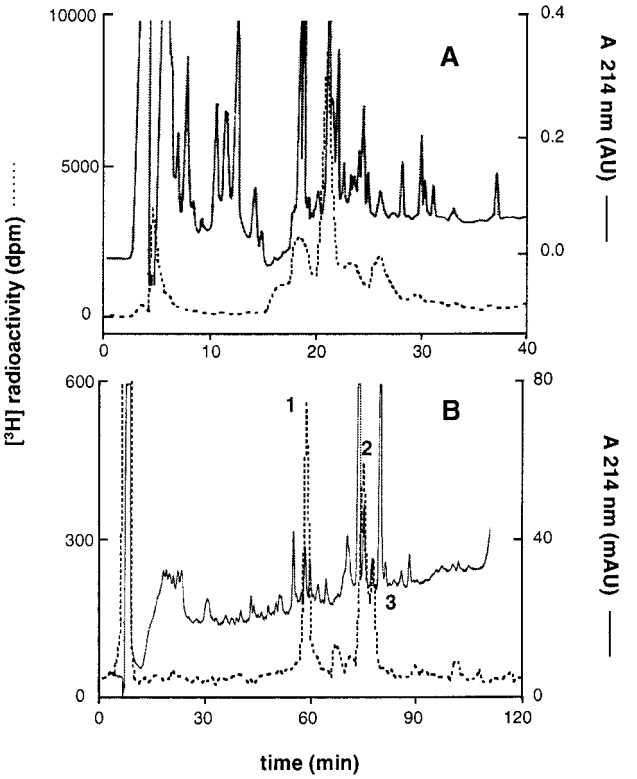

FIGURE 5: HPLC purification steps of [^{3}H]DDF-photolabeled peptides. After irradiation of BuChE in the presence of [^{3}H]DDF (100 μM, 1 Ci/mmol), samples were deglycosylated and digested by trypsin. (A) Digests were applied onto a cation-exchange column and eluted with a NaCl gradient as described in Materials and Methods. (B) Major radioactive peak from cation-exchange chromatography was further loaded onto a C18 reversed-phase column and purified with an acetonitrile gradient.

Table 1: Amino Acid Sequences from the Purified Peptides

peak	sequence
1	T_{315}QILVGVNKDEGTAFLV**Y**G...
2	Y_{61}ANSCCQNIDQSFPGFHG**S**EM**W**NP...
3	Y_{61}ANSCCQNIDQSFPGFHGSEM**W**NP...

DISCUSSION

Photoaffinity labeling experiments are used to bring structural information on ligand binding sites of biological receptors in solution. DDF (*25*), a small aromatic diazonium salt, has been intensively used to map the acetylcholine binding site on different cholinergic proteins (*12*). This probe combined remarkable photochemical properties to a striking mimic of quaternary ammonium salts for cation/π interactions with aromatic amino acid residues. As a new example, the photolabeling of BuChE using the probe [^{3}H]-DDF allowed us to identify two aromatic amino acid residues, Trp82 and Tyr332. This labeling reaction is protectable by tacrine (Figure 2) as well as by tetramethylammonium (*20*). The identification of the labeled amino acids could be assessed by microsequencing of the major labeled peptides (Table 1) which were initially purified to homogeneity by means of HPLC (Figure 5). Importantly, a complete deglycosylation of the labeled protein (Figure 2B) was very helpful in reducing substantially the complexity of the peptide mixture allowing the purification first to proceed successfully and second to identify by MS, directly on the crude tryptic fragments, the peptide Tyr61-Lys103 as being labeled by the probe (Figures 3 and 4).

BuChE, despite its strong sequence homology with AChE, differs markedly from it, in substrate specificity and sensivity (*1*). Considering the different aromatic amino acid residues involved in the binding of quaternary ammonium in the AChE active site (Trp84 and Phe330) and peripheral site (Trp279, Tyr70, and Tyr121), only Trp82(84)[2] is conserved in BuChE, leading to the disruption of the peripheral site of BuChE (*11*). This outcome was confirmed by a series of site-directed mutagenesis experiments, performed on either AChE or BuChE, and consisting mainly of the interchange of the aligned corresponding amino acids (*8, 11, 29*−*31*). Interestingly, a mouse AChE peripheral site triple mutant, Y72(70)N, Y124(121)Q, W286(279)A, produced a protein which affected the binding of AChE peripheral site ligands much more strongly when compared to the difference between AChE and BuChE (*30*). The possibility that binding of the peripheral probes at a different locus in AChE and BuChE has been evoked to explain this difference.

The structure−function relationship of BuChE has been studied mainly through site-directed mutagenesis, molecular modeling, and molecular dynamics experiments (*32*−*35*) based on the 3D model of BuChE (*11*). The studies, which were directly oriented to the structural characterization of the ammonium binding sites, determined the contribution of residues Trp82(84) and Asp70(72) to be the predominant residues for the active and peripheral sites, respectively. While the Trp82(84) was easily identified as the key residue for the ammonium binding at the active site, correlating the situation in AChE, the characterization of the peripheral site, was more problematic due notably to the absence of the representative aromatic residues from the AChE PAS (*11*). A series of publications referred to Asp70(72) as the key amino acid residue for the PAS on BuChE (*33, 34*). The negative charge of the aspartic residue at the rim of the gorge was described as being primarily responsible for the binding of positively charged ligands through ion pair interaction. A three-step binding process successively implying Asp70 and Trp82, and eventually both residues for bis-quaternary ammonium, has been proposed to rationalize the functioning of this enzyme (*34*).

The photogeneration, in our labeling experiment, of a hyper-reactive aryl cation (*36*) allows the exclusion of the fact that such a cationic species diffuses out from a target binding site. According to the measured distance between the two residues Trp82 and Typ332, about 10 Å referring to the BuChE model (*11*), their labeling must result from the occupancy of the DDF probe at two different binding sites. The protection of the labeling reaction by positively charged cholinergic molecules indicates that DDF targeted the quaternary ammonium binding areas of BuChE. Importantly, the observed stoichiometry of labeling of one molecule of probe per active site of BuChE indicates that the labeling at the two ammonium binding sites is mutually exclusive as was the case for the labeling of AChE with DDF (*3*).

Our labeling results first confirm the contribution of Trp82 for the binding of quaternary ammonium at the active site

[2] By convention, the number in parentheses immediately following an amino acid residue refers to the corresponding amino acid residue number in *Torpedo californica* acetylcholinesterase.

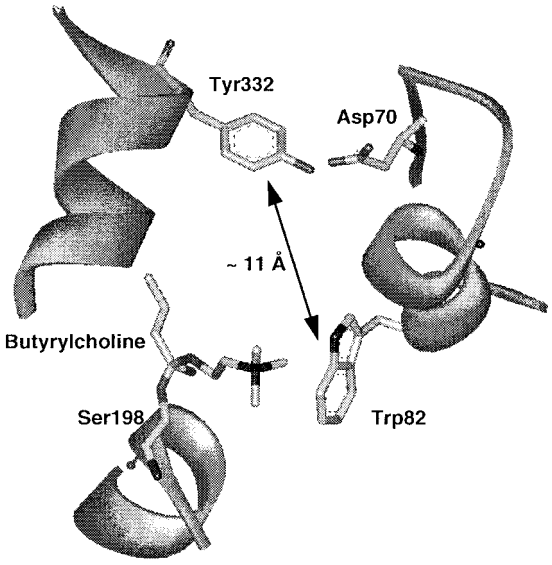

FIGURE 6: Representation of DDF-labeled residues on human BuChE. Trp82 and Tyr332 are shown on a model with docked butyrylcholine (*11*).

and, second, allow us to propose Tyr332 as a predominant residue from the PAS of BuChE to bind quaternary ammonium salts (Figure 6). Interestingly, this residue Tyr332-(334) has been shown to interact directly through a hydrogen bond with Asp70(72) both in the 3D X-ray structure of AChE (*2*) and in the 3D model of BuChE (*11*). This hydrogen bond allows this residue to be indirectly connected to the flexible omega-loop Cys65(67)-Cys92(94) which has been proposed to regulate the functioning of this protein (*34*). Noteworthy, the cation/π interactions involving tyrosine residues have been shown to be dependent on the existence of hydrogen bonds, implying that the tyrosyl hydroxyl group (*37*) leads to a strongly increased cation/π interaction when existing.

In human AChE, Tyr341(334) residue has been shown to be part of a signal relay from the gorge surface to the catalytic center (*38*) while it has been demonstrated, by site-directed mutagenesis, to affect the binding of bis-quaternary ligands such as BW284C51 and decamethonium (*31*, *39*). Interestingly, the 3D X-ray structure of the mouse AChE complexed with fasciculin revealed, by comparison with the 3D *Torpedo* AChE structure, that after fasciculin binding, the largest conformational motion was observed for residue Tyr341(334) (*6*). However, one should keep in mind that AChE and BuChE are different proteins and the results obtained for the binding of fasciculin on AChE might not be relevant for BuChE. The only study which has been achieved on BuChE Tyr332 residue used the Y332F mutant to evaluate the importance of the hydrogen bond between Tyr332 and Asp70 for the binding of quaternary ammonium ligands (*34*). A moderate decrease in binding affinities of mono- and bis-quaternary ammonium derivatives was observed; however, the Y332F mutant did not abolish the cation/π interaction of this residue and additional mutagenesis experiments are required to delineate accurately the importance of Tyr332 in the binding of quaternary ammonium ligands. Although the residue Asp70 was not part of the major labeled peptides by [^{3}H]DDF, we cannot rule out its labeling completely; either it could have been present in minor radiolabeled peptide fragments or the labeling might have been partially lost during the used experimental procedures (i.e., aqueous formic acid treatment during microsequencing). Therefore, the involvement of both residue Asp70 and residue Tyr332 for the binding of quaternary ammonium at the PAS of BuChE is conceivable (Masson, personal communication).

The existence of a PAS at BuChE has been questioned (*11*), due notably to the absence of specific ligands for this site. Evidently, if the BuChE PAS exists, it is structurally very different from the AChE PAS (see above), and this is best illustrated by the striking difference in binding affinities of fasciculin, an AChE peripheral site ligand, for these two proteins (*40*). Our labeling results, besides identifying the well-characterized Trp82 at the active site of BuChE, strongly reinforce the existence of a peripheral site on this protein by identifying Tyr332 as a major participant. This result confirms a complete different location in the 3D structures of the peripheral sites of AChE and BuChE. Work is currently in progress to determine precisely the structural determinants and functional implications of the BuChE peripheral site.

ACKNOWLEDGMENT

We are grateful to Dr P. Bulet (UPR CNRS 9022, Strasbourg) for sequence analysis as well fruitful discussions.

REFERENCES

1. Massoulie, J., Pezzementi, L., Bon, S., Krejci, E., and Vallette, F. M. (1993) *Prog. Neurobiol. 41*, 31−91.
2. Sussman, J. L., Harel, M., Frolow, F., Oefner, C., Goldman, A., Toker, L., and Silman, I. (1991) *Science 253*, 872−879.
3. Harel, M., Schalk, I., Ehret-Sabatier, L., Bouet, F., Goeldner, M., Hirth, C., Axelsen, P. H., Silman, I., and Sussman, J. L. (1993) *Proc. Natl. Acad. Sci. U.S.A. 90*, 9031−9035.
4. Harel, M., Kleywegt, G. J., Ravelli, R. B., Silman, I., and Sussman, J. L. (1995) *Structure 3*, 1355−1366.
5. Harel, M., Quinn, D. M., Nair, H. K., Silman, I., and Sussman, J. L. (1996) *J. Am. Chem. Soc. 118*, 2340−2346.
6. Bourne, Y., Taylor, P., and Marchot, P. (1995) *Cell 83*, 503−512.
7. Sussman, J. L., and Silman, I. (1992) *Curr. Opin. Struct. Biol. 2*, 721−729.
8. Taylor, P., and Radic, Z. (1994) *Annu. Rev. Pharmacol. Toxicol. 34*, 281−320.
9. Dougherty, D. A., and Stauffer, D. A. (1990) *Science 250*, 1558−1560.
10. Dougherty, D. A. (1996) *Science 271*, 163−168.
11. Harel, M., Sussman, J. L., Krejci, E., Bon, S., Chanal, P., Massoulie, J., and Silman, I. (1992) *Proc. Natl. Acad. Sci. U.S.A. 89*, 10827−10831.
12. Kotzyba-Hibert, F., Kapfer, I., and Goeldner, M. (1995) *Angew. Chem., Int. Ed. Engl. 34*, 1296−1312.
13. Schumacher, M., Camp, S., Maulet, Y., Newton, M., MacPhee-Quigley, K., Taylor, S. S., Friedmann, T., and Taylor, P. (1986) *Nature 319*, 407−409.
14. Kieffer, B., Goeldner, M., Hirth, C., Aebersold, R., and Chang, J. Y. (1986) *FEBS Lett. 202*, 91−96.
15. Kreienkamp, H. J., Weise, C., Raba, R., Aaviksaar, A., and Hucho, F. (1991) *Proc. Natl. Acad. Sci. U.S.A. 88*, 6117−6121.
16. Schalk, I., Ehret-Sabatier, L., Bouet, F., Goeldner, M., and Hirth, C. (1992) in *Multidisciplinary Approaches to Cholinesterase Functions* (Shafferman, A., and Velan, B., Eds.) pp 117−120, Plenum Press, New York.
17. Schalk, I., Ehret-Sabatier, L., Bouet, F., Goeldner, M., and Hirth, C. (1994) *Eur. J. Biochem. 219*, 155−159.
18. Haas, R., Adams, E. W., Rosenberry, T. L., and Rosenberry, T. L. (1992) in *Multidisciplinary Approaches to Cholinesterase*

Functions (Shafferman, A., and Velan, B., Eds.) pp 131−139, Plenum Press, New York.
19. Schalk, I., Ehret-Sabatier, L., Le Feuvre, Y., Bon, S., Massoulie, J., and Goeldner, M. (1995) *Mol. Pharmacol. 48*, 1063−1067.
20. Ehret-Sabatier, L., Schalk, I., Goeldner, M., and Hirth, C. (1992) *Eur. J. Biochem. 203*, 475−481.
21. Rosenberry, T. L., and Bernhard, S. A. (1971) *Biochemistry 10*, 4114−4120.
22. Autelitano, F., Weill, C., Goeldner, M., and Ilien, B. (1997) *Biochem. Pharmacol. 53*, 501−510.
23. Lockridge, O., and LaDu, B. N. (1978) *J. Biol. Chem. 253*, 361−366.
24. Ellman, G. L., Courtney, K. D., Andres, J. V., and Featherstone, R. M. (1961) *Biochem. Pharmacol. 7*, 88−95.
25. Goeldner, M. P., and Hirth, C. G. (1980) *Proc. Natl. Acad. Sci. U.S.A. 77*, 6439−6442.
26. Laemmli, U. K. (1970) *Nature 227*, 680−685.
27. Ravanat, C., Morales, M., Azorsa, D. O., Moog, S., Schuler, S., Grunert, P., Loew, D., van Dorsselaer, A., Cazenave, J. P., and Lanza, F. (1997) *Blood 89*, 3253−3262.
28. Lockridge, O., Bartels, C. F., Vaughan, T. A., Wong, C. K., Norton, S. E., and Johnson, L. L. (1987) *J. Biol. Chem. 262*, 549−557.
29. Vellom, D. C., Radic, Z., Li, Y., Pickering, N. A., Camp, S., and Taylor, P. (1993) *Biochemistry 32*, 12−17.
30. Radic, Z., Pickering, N. A., Vellom, D. C., Camp, S., and Taylor, P. (1993) *Biochemistry 32*, 12074−12084.
31. Barak, D., Kronman, C., Ordentlich, A., Ariel, N., Bromberg, A., Marcus, D., Lazar, A., Velan, B., and Shafferman, A. (1994) *J. Biol. Chem. 269*, 6296−6305.
32. Loewenstein-Lichtenstein, Y., Glick, D., Gluzman, N., Sternfeld, M., Zakut, H., and Soreq, H. (1996) *Mol. Pharmacol. 50*, 1423−1431.
33. Masson, P., Froment, M. T., Bartels, C. F., and Lockridge, O. (1996) *Eur. J. Biochem. 235*, 36−48.
34. Masson, P., Legrand, P., Bartels, C. F., Froment, M. T., Schopfer, L. M., and Lockridge, O. (1997) *Biochemistry 36*, 2266−2277.
35. Saxena, A., Redman, A. M., Jiang, X., Lockridge, O., and Doctor, B. P. (1997) *Biochemistry 36*, 14642−14651.
36. Gasper, S. M., Devadoss, C., and Schuster, G. B. (1995) *J. Am. Chem. Soc. 117*, 5206−5211.
37. Mecozzi, S., West, A. P., Jr., and Dougherty, D. A. (1996) *Proc. Natl. Acad. Sci. U.S.A. 93*, 10566−10571.
38. Shafferman, A., Velan, B., Ordentlich, A., Kronman, C., Grosfeld, H., Leitner, M., Flashner, Y., Cohen, S., Barak, D., and Ariel, N. (1992) *EMBO J. 11*, 3561−3568.
39. Velan, B., Barak, D., Ariel, N., Leitner, M., Bino, T., Ordentlich, A., and Shafferman, A. (1996) *FEBS Lett. 395*, 22−28.
40. Radic, Z., Duran, R., Vellom, D. C., Li, Y., Cervenansky, C., and Taylor, P. (1994) *J. Biol. Chem. 269*, 11233−11239.

BI980536L